Peculiar Geological Features in the Nugget Sandstone of the Moxa Arch

Dhruv Agrawal, Brady Lujan, Sumit Verma, The University of Texas of the Permian Basin*
Subhashis Mallick, The University of Wyoming

Summary

The Green River Basin in the SW Wyoming is responsible for all production within Lincoln, Sublette, Sweetwater, and Uinta Counties in Wyoming. This study focuses on peculiar features in the Lincoln County, we call them FLTs (funny looking things), observed in the seismic data associated with the Triassic/Jurassic deposition in the Moxa Arch. The acquisition and processing errors cannot explain these features, which led us to look for a geologic explanation. Well to seismic ties on three wells surrounding the seismic survey indicated that the observed FLTs on seismic correspond to the Jurassic aged Nugget Sandstone formation. Based on the seismic inversion and the petrophysical model, we concluded that the lithology distribution is comprised of dunal and inter-dunal deposits.

Introduction

Different seismic attributes can concentrate and better interpret different geological and stratigraphic features in the geology of an area. For example, amplitude and frequency attributes can show stratigraphic changes, on the other hand, geometric attributes such as dip, curvature and convergence are better for finding out reflector morphology. Similarly, while some seismic attributes are better indicators of edges of seismic facies, others are the optimum choices for measuring the facies themselves (Chopra and Marfurt, 2007).

While looking at different seismic attributes used to be good enough in earlier days, with the recent developments in computational geophysics, multiple attributes can be layered or co-rendered over each other to be able to visualize or identify a seismic facie that would have otherwise gone unnoticed by even the best of geology interpreters (Roy et al., 2013; Zhang et al., 2015; Zhao et al., 2016). We begin our paper by discussing the geology of the Moxa Arch, followed by the description of the available data. Then we will explain the seismic attributes we used along with well to seismic tie, seismic inversion and co-rendering them together. We conclude with our interpretation based on the results we got and the analog formation from the South..

Geology of the study area

The Moxa Arch, a doubly plunging anticline formed during early stage of Laramide orogeny, is located to the west of Green River Basin and Rock Springs Uplift. It dips gently (~5 degrees) and extends from beneath the Uinta Mountains at the Utah/Wyoming border, north to the town of La Barge, Wyoming, where it turns northwest and plunges beneath the western Wyoming fold-and-thrust belt. Wyoming thrust belt developed during Laramide orogeny has a well-documented structural history that indicates uplift along a basement-involved thrust fault beginning in the Late Cretaceous and continuing through the early Eocene (Campbell-Stone et al., 2011, Verma et al., 2016). Because of its size and structural closure, the Moxa Arch has been the target of extensive hydrocarbon exploration since the 1960s with major gas and oil reservoirs being discovered all along the arch.

In this study, we focus on the structures of the Moxa Arch based on seismic attributes and seismic inversion. One of such formations that harbors the seismic structures in question is the Nugget Sandstone that shows minimal faulting in formation, regional unconformity at the top and base and is of Lower Jurassic in age (Picard, 1997).

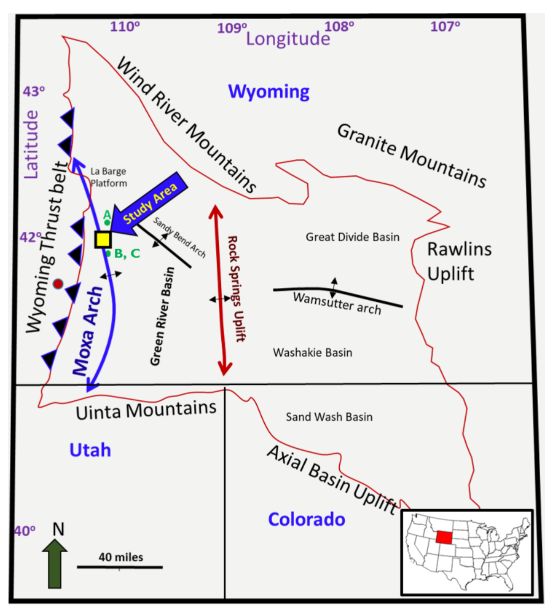

Figure 1. Location map of the Moxa Arch and Rock Springs Uplift in SW Wyoming (modified after Verma et al., 2016). A, B and C are the wells used for the study.

10.1190/segam2018-2996490.1

Seismic and well log data

The area of the 3D seismic survey is about 93.2 km^2 or 36 mi^2. Since, there are no wells in the area with the seismic data which are deep enough to penetrate the Nugget Sandstone we are interested in, we used the three wells surrounding the seismic data section (Figure 2). The low dip and continuity of the late Paleozoic (deeper) and the Mesozoic (shallower) formations, without a large scale heterogeneity, allows us to use the above mentioned wells for the well to seismic tie.

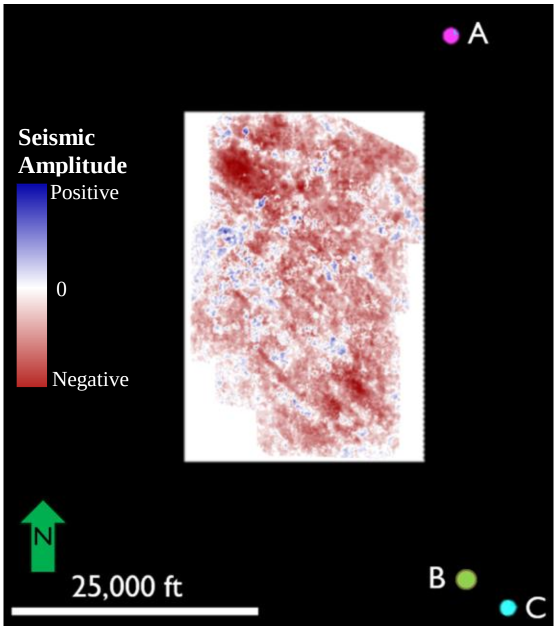

Figure 2. Locations of wells A, B and C relative to the seismic survey area. Seismic amplitude time slice at 1 sec.

Seismic attribute analysis

Coherence

Coherence is one of the most common seismic attribute used to identify faults, channels or other discontinuous features on a surface. It represents the similarity or continuity between two points. If two neighboring points are similar/continuous to each other then coherence is 1, if they're completely dissimilar then the value is 0. It is used to map the lateral extent of a formation.

Structural curvature

Mathematically, the structural curvature equals the rate of change in the dip of a surface. If the dip continues to increase (anticline), the curvature will be positive. Similarly a continuous decrease in the surface dip (syncline) leads to negative curvature and a constant dip (flat surface) denotes 0 curvature. The curvature is used to represent the shape of the surface. Every single point on a 3D surface has 2 principal curvatures denoted by k_1 and k_2 which are called the maximum and minimum values of the curvature respectively.

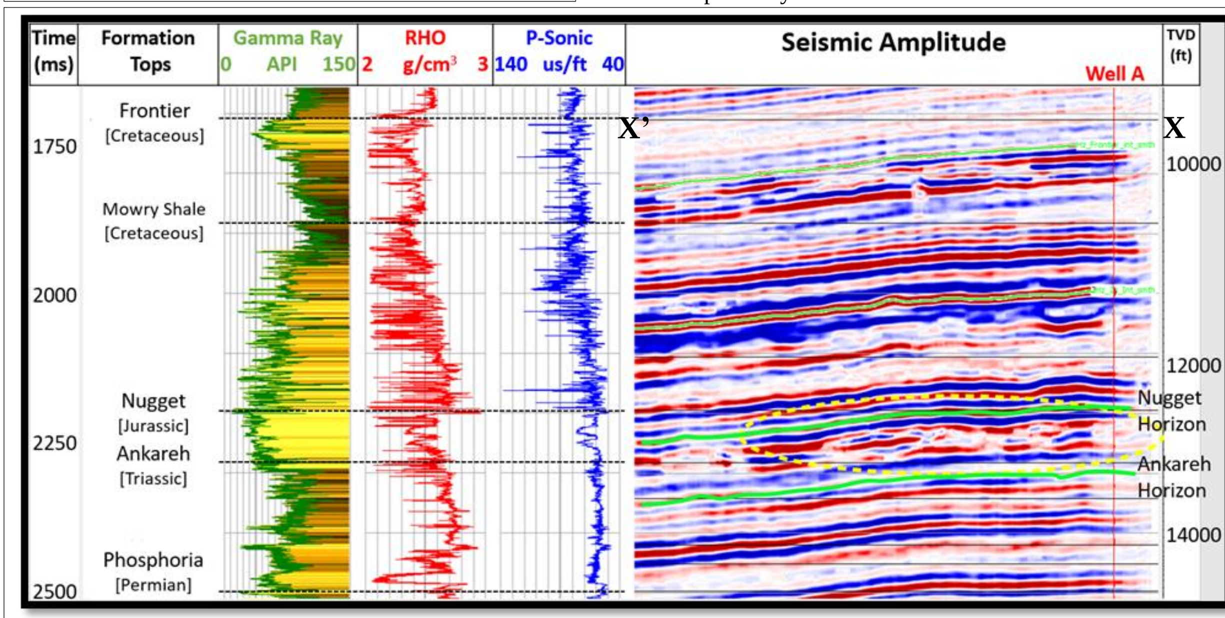

Figure 3. Well to seismic tie – Well A. Well A highlighted as red vertical line. The yellow ellipse exhibits the structures we are interested in.

10.1190/segam2018-2996490.1

It is important to note that the shapes represented by different curvature values depend on the wavelength of the data we want to look at. A syncline for small wavelength can be a part of a bigger anticline (longer wavelength). The combination of k_1 and k_2 may represent different shapes of the surface like dome, valley, ridge or bowl etc. (Roberts, 2001; Bergbauer et al., 2003; Al-Dossary and Marfurt, 2006). The mean curvature is calculated by averaging k_1 and k_2.

Well to seismic tie

To do the well to seismic tie, we moved the wells to the nearest possible location into our 3D seismic survey. The 2 horizons picked capturing the FLTs (inside yellow ellipse) we are interested in, turned out to be the boundaries of the Nugget Sandstone as can be seen in the well to seismic tie of Well A (Figure 3). The peculiar features are spread over the thickness of about 1500 feet from the depth of 12,500 ft to 14,000 ft between the 3 wells.

The low gamma ray log values in the Nugget Sandstone indicate the presence of sands in the formation.

Co-rendering seismic attributes

Figure 4 shows the coherence and coherence corendered with curvature, of the Nugget Sandstone after flattening it with respect to the Nugget horizon itself to look into the stratigraphical features in the area. In our case here, the coherence attribute confirms the presence of miniature discontinuities and the curvature attribute confirms the presence of anticlines and synclines surrounding those discontinuities.

We further did seismic inversion on the data and got P-impedance values for our area of interest. While co-rendering P-impedance with coherence (Figure 5), it can be seen that the small structures delineated by coherence are filled with low P-impedance values (light green to bright yellow to red), possibly cleaner sands, and are surrounded by high impedance values (blue to light blue colors) which might be limey to shaly siltstones.

We think that the sands can be characterized as the dune sands while the limey/shaly siltstones can be interpreted as inter-dunes.

Conclusions

The Nugget Sandstone is an eolian deposit and is equivalent to the Navajo sandstone. It is characterized by dunal facies comprised mainly of cross stratified eolian sands and inter-dunal facies characterized by thin horizontal lenticular beds. The time/depth correlation confirms that the FLTs seen in the seismic data are within the Nugget Sandstone, as seen in the seismic to well tie. Seismic interpretation further helps to discriminate the lithology distribution into dunal and inter-dunal deposits. Therefore the FLTs seen in our data are most likely to be dune deposits surrounded by inter-dunal deposits within the Nugget Sandstone. Further seismic analysis would be needed; thin-bed tuning especially, to interpret the exact lithology in the inter-dunal areas of the Nugget.

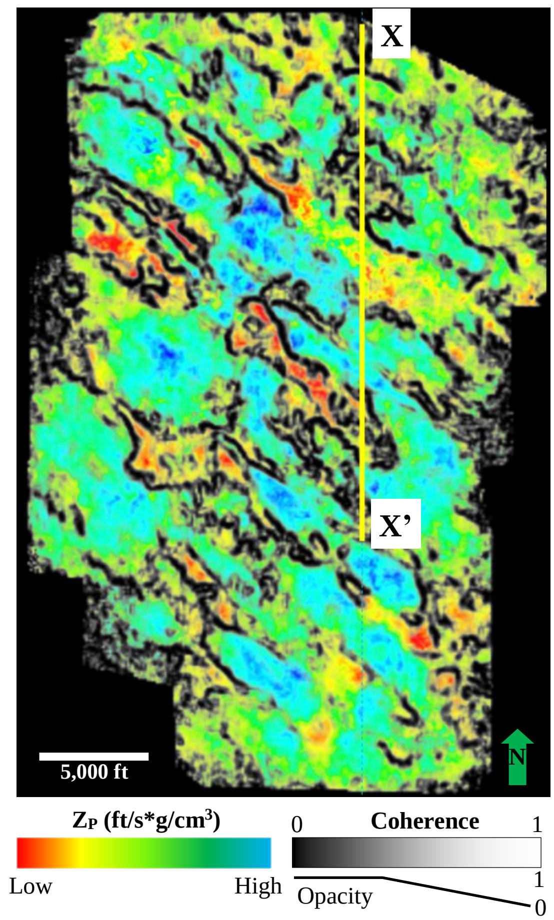

Figure 5. Stratal slice (44 ms below Nugget) of Coherence and P-Impedance (Z_P). A co-rendering of coherence and inversion shows the cleaner sands (low impedance, light green to bright yellow to red) are in the structures delineated by coherence. These sands may be characterized as the dune sands while the areas in the blue to light blue colors (high impedance) show the areas with the limey to shaly siltstones and can be interpreted as the inter-dunes.

Acknowledgement

Thanks to Attribute Assisted Processing and Interpretation consortium for providing AASPI software, which was used to compute seismic attributes. We also thank Schlumberger for Petrel and CGG GeoSoftware for Hampson-Russell software licenses provided to UTPB. The seismic data was obtained with the research grant provided by the United States Department of Energy: Contract No: DE-FE0023328.

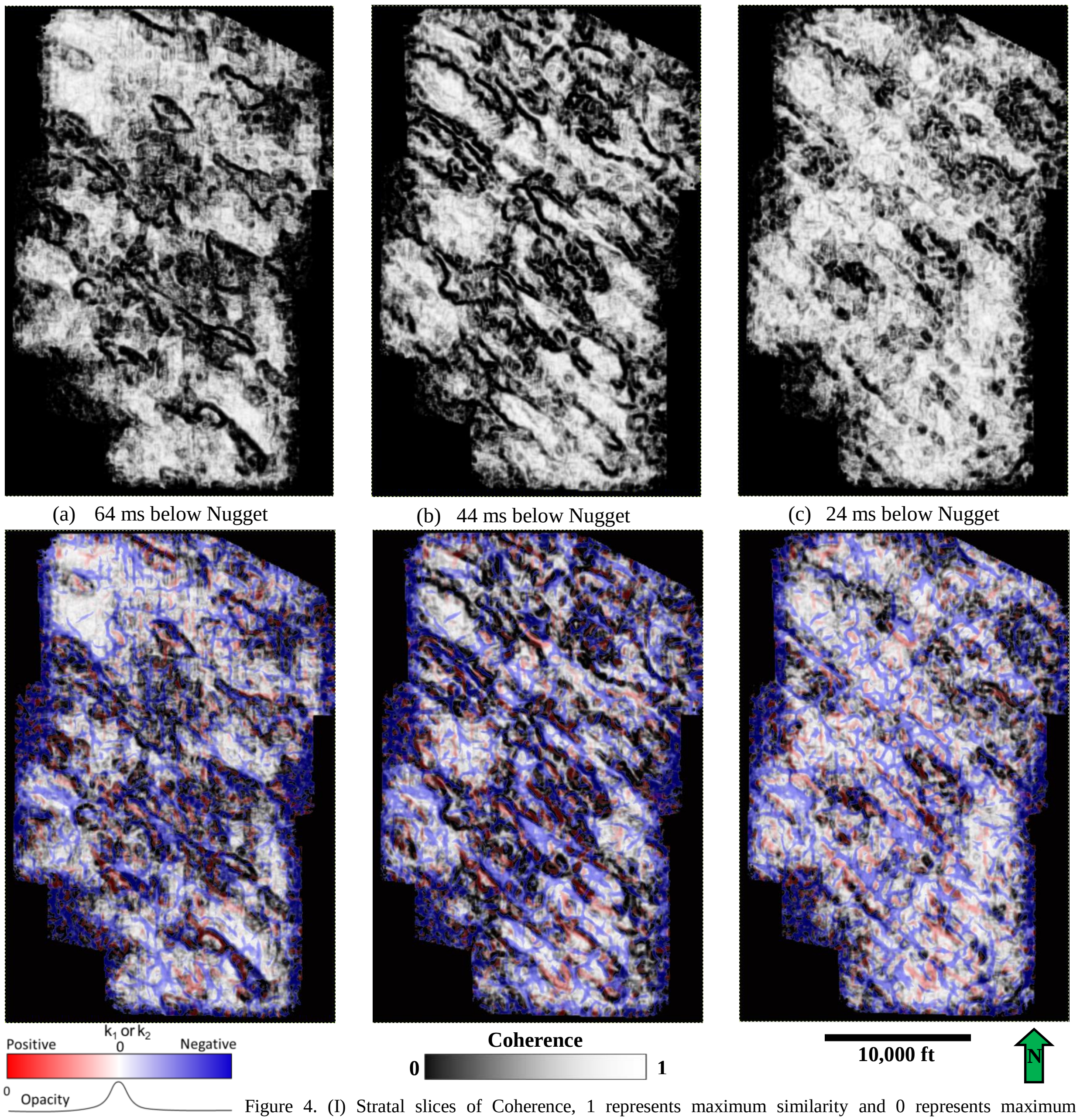

Figure 4. (I) Stratal slices of Coherence, 1 represents maximum similarity and 0 represents maximum dissimilarity, (II) Stratal slices of most positive curvature (k_1) co-rendered with most negative curvature (k_2) and coherence. The above stratal slices were taken after flattening the seismic section with respect to the Nugget horizon at 2226 ms The structures begin to appear 24 ms below Nugget (Fig. c), become prominent (Fig. b) and then start disappearing about 64 ms below Nugget (Fig. a). Coherence determines the lateral changes in the lithology, so these structures are the areas that show discontinuity. The corendered figure implies that the distinct features seen in coherence slices are surrounded by anticlines and synclines.

REFERENCES

Al-Dossary, S., and K. J. Marfurt, 2006, Multispectral estimates of reflector curvature and rotation: Geophysics, **71**, no. 5, P41–P51, https://doi.org/10.1190/1.2242449.

Bergbauer, S., T. Mukerji, and P. Hennings, 2003, Improving curvature analyses of deformed horizons using scale-dependent filtering techniques: AAPG Bulletin, **87**, 1255–1272, https://doi.org/10.1306/0319032001101.

Campbell-Stone, E., R. Lynds, C. Frost, T. P. Becker, and B. Diem, 2011, The Wyoming carbon underground storage project: Geologic characterization of the Moxa Arch and Rock Springs Uplift: Energy Procedia, **4**, 4656–4663, , https://doi.org/10.1016/j.egypro.2011.02.426.

Chopra, S., and K. J. Marfurt, 2007, Seismic attributes for prospect identification and reservoir characterization: SEG.

Picard, M. D., 1997, Mesozoic history of Wyoming: Wyoming State Geological Survey Public Information Circular, **38**, 73–105.

Roberts, A., 2001, Curvature attributes and their application to 3D interpreted horizons: First Break, **19**, 85–100, https://doi.org/10.1046/j.0263-5046.2001.00142.x.

Roy, A., B. L. Dowdell, and K. J. Marfurt, 2013, Characterizing a Mississippian tripolitic chert reservoir using 3D unsupervised and supervised multiattribute seismic facies analysis: An example from Osage County, Oklahoma: Interpretation, **1**, SB109–SB124, https://doi.org/10.1190/INT-2013-0023.1.

Verma, S., E. Campbell-Stone, H. Sharma, S. Mallick, and D. Grana, 2016, Seismic attribute illumination of the Moxa Arch: A probable site for carbon sequestration: 86th Annual International Meeting, SEG, Expanded Abstracts, 1874–1878, https://doi.org/10.1190/segam2016-13953191.1.

Zhang, B., T. Zhao, X. Jin, and K. J. Marfurt, 2015, Brittleness evaluation of resource plays by integrating petrophysical and seismic data analysis: Interpretation, **3**, T81–T92, https://doi.org/10.1190/INT-2014-0144.1.

Zhao, T., J. Zhang, F. Li, and K. J. Marfurt, 2016, Characterizing a turbidite system in Canterbury Basin, New Zealand, using seismic attributes and distance-preserving self-organizing maps: Interpretation, **4**, no. 1, SB79–SB89, https://doi.org/10.1190/INT-2015-0094.1.